TEM STUDIES OF THE W PHASE AND ITS ORDERED W′ PHASE IN RARE EARTH Mg ALLOYS①

Luo, Zhiping Zhang, Shaoqing
Beijing Institute of Aeronautical Materials, Beijing 100095, China
Tang, Yali
Zhengzhou Institute of Technology, Zhengzhou 450002, China

ABSTRACT

By means of transmission electron microscopy (TEM), the W phase and its ordered W′ phase in as-cast Mg-Zn-Zr-Y system alloys were studied. The W phase, which distributes along the grain boundaries in the form of a lamellar eutectoid with Mg, is of *FCC* structure with $a = 0.865$ nm. The W′ phase, which is an ordered structure of the W phase with $a = 2.055$ nm, was found in the alloy with lower Y content. The W and W′ phases have a simple orientation relationship of $(100)_W // (100)_{W'}$, $(010)_W // (010)_{W'}$, and $(001)_W // (001)_W$; but they do not have an orientation relationship with the α-Mg matrix. The results of convergent electron diffractions (CBD) on these phases show that their point group is $m3m$ and that the space group is $Fm3m$.

Key words: Mg alloy rare earth phase TEM

1 INTRODUCTION

Mg alloys have found many applications over a long period of time[1-3]. However, the microstructtural studies of Mg alloys have been limited[1-6]. In the recent years, the phase strucures of Mg-Zn(-Zr)-RE alloys have been identified because of the high strength of this system of alloys[7-11]. The W phase[7-10], Z phase[7-10] and the X phase[7-9,11], have been identified mainly by X-ray diffraction. In the present paper electron microscopy studies are made on the W phase, and a new ordered structure of the W phase, which is denoted as W′ phase, is found. Their point group and space group are obtained by convergent beam diffraction (CBD).

2 EXPERIMENTAL METHODS

Two cast alloys with Mg-5.63 Zn-0.49 Zr-3.45 Y (alloy A) and Mg-5.56 Zn-0.47 Zr-1.72 Y (alloy B) weight percent compositions were used. The TEM thin foils were prepared by twin-jet polishing (For details see reference[5]). The experiments were conducted on a JEM-2000FX analytical electron microscope with side-inserting double-tilting specimen stage at a working voltage of 120 kV. An IBM/PC computer was used for indexing selected area diffraction (SAD) patterns from monocrystals and matrix calculations. The camera length $L\lambda$ was accurately measured from the rings diffracted by polycrystalline MgO.

① Manuscript received Nov. 21, 1992

3 EXPERIMENTAL RESULTS AND ANALYSES

3.1 *Appearances and Crystal Structures of the* W *and* W' *phases*

In alloy A with high Y content, the rare earth compound is the W phase. As shown in Fig. 1, the W phase distributes along the grain boundaries in the form of a lamellar eutectoid. The SAD confirms that it is a *FCC* sturcture with $a = 0.685$ nm. Fig. 2 shows the bright field(BF) image and central dark field(CDF)image by $(220)_W$ reflection from the W phase.

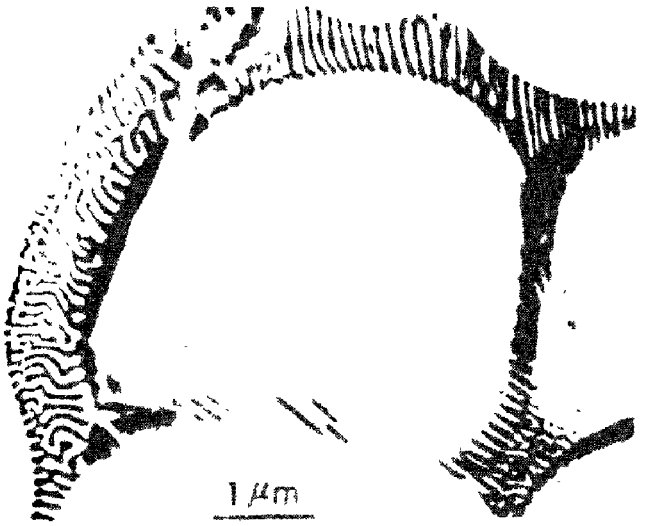

Fig. 1 Appearance of grain boundary W phase in alloy A

In the alloy B with lower Y content than alloy A, an ordered structure of the W phase was found. Fig. 3 shows the appearance of the grain boundary rare earth phase in this aloy; it is just the same as that in alloy A. However the SAD with small field limiting apertures revealed that there are different structures in region B, as demarcated by white dotted lines in Fig. 3, and in region A. In order to search the crystal zones with low indeces, this field was tilted at large angles along the direction of the Kikuchi bands in the DIFF model. Fig. 4 shows the standard Kikuchi triangle composed of three crystal zones with low indeces from regions A and B. It is found that region A is the W phase *FCC* structure. However, the SAD patterns from in all three directions are one-third of the W phase, i. e. $g_{100} = (1/3)\, g_{100W}$, $g_{010} = (1/3)\, g_{010W}$ and $g_{001} = (1/3) g_{001W}$. Thus, the three basic lattice vectors should be three times larger than those of the W phase, i. e. $a = 3\, a_W$, $b = 3\, b_W$, and $c = 3\, c_W$. Therefore, the structure of the region B is an ordered structure of the region A. This ordered structure is also of *FCC* structure, but its parameter is three times larger than that of the W phase, i. e. $a_{W'} = 2.055$ nm. This kind of structure has not been reported before, we denote it as the W' phase in this paper. From the SAD patterns in Fig. 4, it is evident that the W and W' phases have simple orientation relationship as follows: $(100)_W // (100)_{W'}$, $(010)_W // (010)_{W'}$ and $(001)_W // (001)_{W'}$.

In the alloy B, the separated W' phase is also observed, as shown in Fig. 5(a). Its corresponding [111] zone pattern is shown in Fig. 5(b).

3.2 *Orientation Relationship Between the Matrix and* W *or* W' *Phase*

Tilting the specimen according to the Bragg position of the W phase, a series of SAD patterns of the W phase and matrix are obtained. However, it is difficult to find a close parallel, i. e. the coincident reciprocal points crystal planes, with low indeces of the two phases. Fig. 6 shows the SAD patterns of the two phases in the $[111]_W$, $[112]_W$ and $[011]_W$ zones. Considering the 180° uncertainty for indexing of the SAD patterns, the approximately parallel planes of the two phases are measured from the patterns, and their crystal direction transfor-

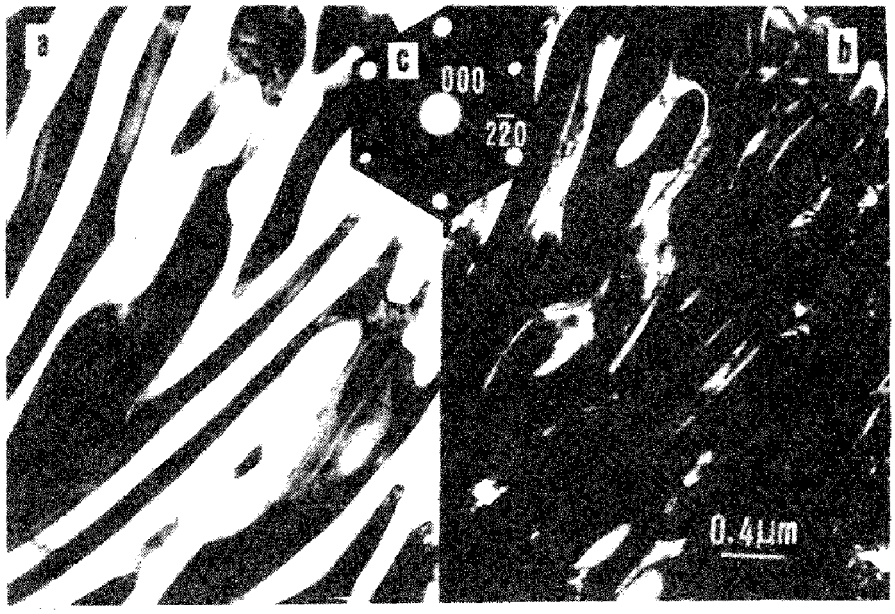

Fig. 2 Grain boundary W phase in alloy A

(a)—BF image; (b)—CDF image by $(220)_W$ reflection; (c)—SAD pattern

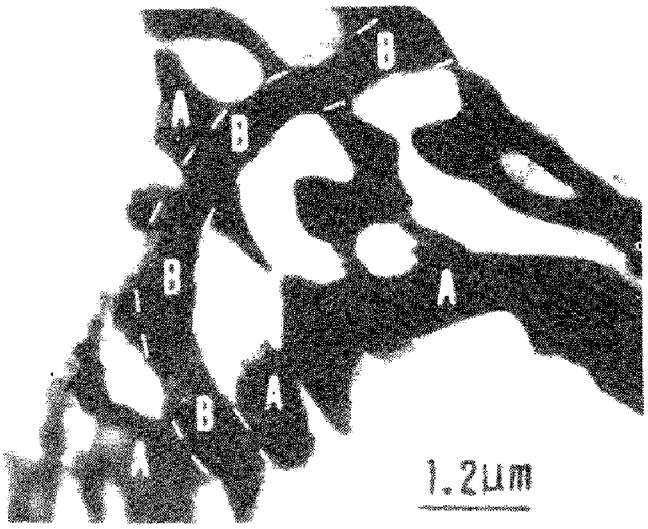

Fig. 3 Rare earth phase in alloy B

mation matrices are calculated as follows:

For Fig. 6(a): $(200)_{Mg}//(-2.495\ 4\ -1.505)_W\ [011]_{Mg}//[111]_W$

$$B_{11}=\begin{bmatrix}-0.143 & -0.121 & 0.637\\ 0.282 & 0.090 & 0.427\\ -0.349 & 0.439 & 0.078\end{bmatrix}$$

$(200)_{Mg}//(2.495-41.505)_W$

$[011]_{Mg}//[111]_W$

$$B_{12}=\begin{bmatrix}0.028 & 0.393 & 0.124\\ -0.422 & 0.182 & 0.335\\ 0.209 & -0.167 & 0.683\end{bmatrix}$$

For Fig. 6(b): $(0-1-2)_{Mg}//(1.047\ 1.953\ -1)_W\ [1-21]_{Mg}//[112]_W$

$$B_{21}=\begin{bmatrix}-0.195 & -0.241 & 0.212\\ 0.274 & -0.311 & -0.485\\ 0.331 & -0.186 & 0.626\end{bmatrix}$$

$(0-1-2)_{Mg}//(-1.047-1.9531)_W$

$[1-21]_{Mg}//[112]_W$

$$B_{22}=\begin{bmatrix}0.404 & -0.017 & 0.064\\ -0.104 & 0.098 & 0.710\\ 0.220 & -0.503 & 0.102\end{bmatrix}$$

For Fig. 6(c): $(0-1-1)_{Mg}//(0.424-22)_W$

$[1-22]_{Mg}//[011]_W$

$$B_{31}=\begin{bmatrix}-0.408 & 0.166 & 0.370\\ 0.105 & -0.437 & 0.201\\ 0.202 & 0.041 & 0.635\end{bmatrix}$$

$(0-1-1)_{Mg}//(-0.4242-2)_W$

$[1-22]_{Mg}//[011]_W$

$$B_{32}=\begin{bmatrix}-0.408 & 0.167 & 0.371\\ 0.115 & -0.437 & 0.201\\ 0.202 & 0.041 & 0.635\end{bmatrix}$$

For Fig. 6(d): $(-212)_{Mg}//(-2.329-1.671\ 1.671)_W$

$[-345]_{Mg}//[011]_W$

$$B_{41}=\begin{bmatrix}0.340 & 0.102 & -0.123\\ -0.038 & -0.090 & -0.743\\ -0.323 & 0.449 & -0.120\end{bmatrix}$$

$(-212)_{Mg}//(2.329\ 1.671-1.671)_W$

$[-345]_{Mg}//[011]_W$

$$B_{42}=\begin{bmatrix}-0.340 & -0.102 & 0.123\\ -0.323 & 0.449 & -0.120\\ -0.038 & -0.090 & -0.743\end{bmatrix}$$

It is found that the absolute values of

the matrix elements of the above matrices are in disagreement with each other. Using Calculations of these matrices show that the W phase and matrix do not have the usual orientation relationship between *HCP-FCC* structures as $<110>_{HCP} // <100>_{FCC}$, and $\{001\}_{HCP} // \{111\}_{FCC}$. Furthermore, calculations of the angles between the W phase zones $<UVW>_W$ and α-Mg matrix zones $<UVW>_{Mg}$ from these SAD patterns show that they are also in disagreement with each other. Using the standard stereographic projection diagram for analyses, it is found that the projections of the two phases cannot coincide in the diagram. Thus it can be concluded that the W phase and W′ phase have no orientaion relationships with the matrix. As shown in Fig. 6(c) and 6(d), two α-Mg zones are present together with the [011] zone of the W phase. This is the result of having no orientation relationship other than kinds of orientation relationships.

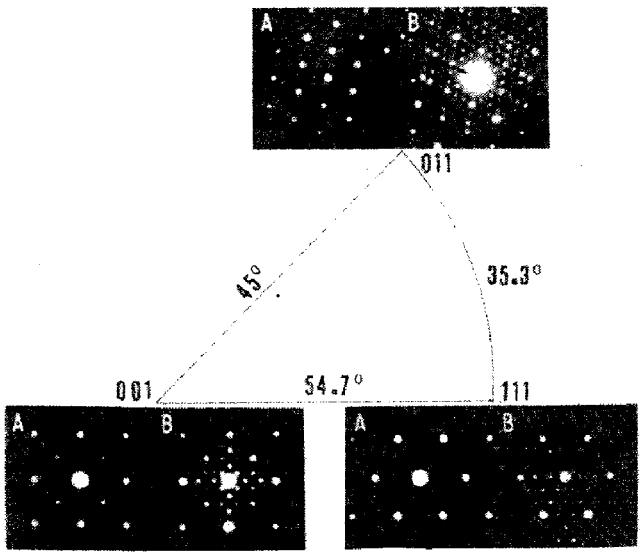

Fig. 4 SAD patterns from regions A and B in Fig. 3 by tilting

3.3 *Point Group and Space Group of* W *and* W′ *phases*

Fig. 7 shows the CBD patterns in the [111] and [011] zones of the W phase. According to the [111] zone pattern in Fig. 7 (a), it can be seen that the whole pattern (WP) symmetry is $3m$. Correspondently, its possible diffraction point groups are $3m$, $3ml_R$ and 6_Rmmm_R. Among them, only the 6_Rmmm_R and $3m$ diffraction point groups accord with the [111] zone for cubic structure, they correspond to the $m3m$ and $43m$ point groups respectively[12]. According to the [011] pattern in Fig. 7(b), its whole pattern symmetry is $2mm$, which corresponds to possible $2mm$, $2mm1_R$ and 4_Rmm1_R diffraction groups, but only 4_Rmm1_R diffraction group accords with the [011] zone for cubic structure, which corresponds to the $m3m$ point group. Therefore, the point group of the W phase is $m3m$.

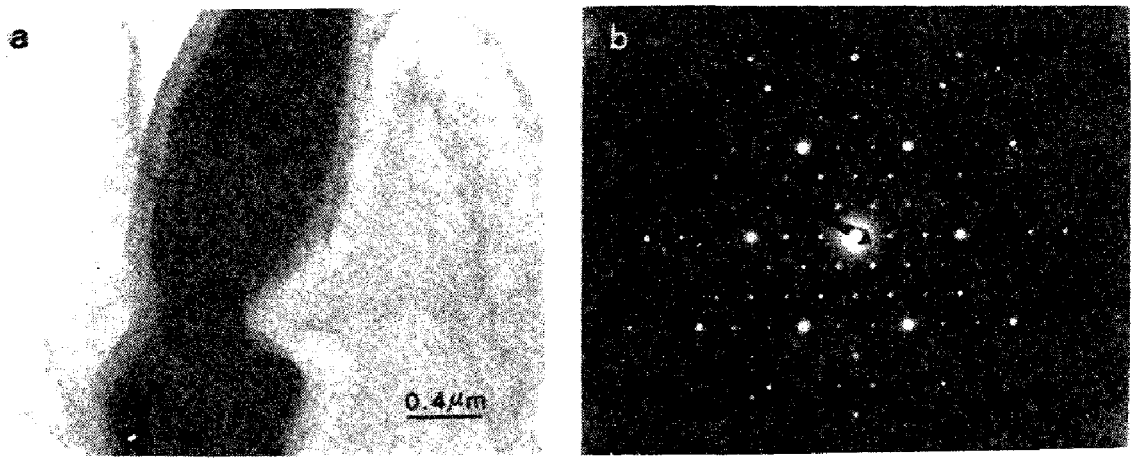

Fig. 5 Massive W′ phase a and its [111] zone diffraction pattern (b) in alloy B

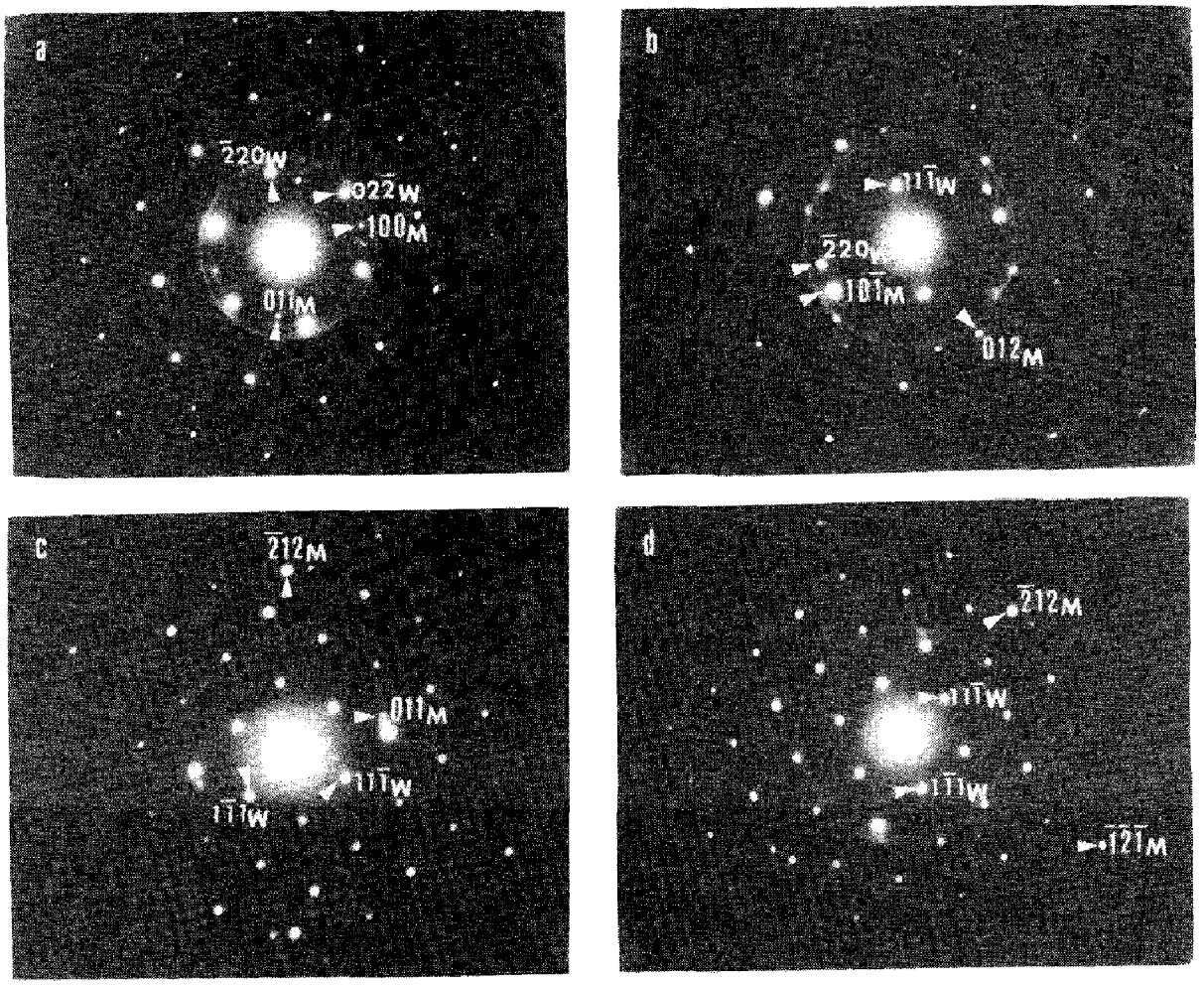

Fig. 6 SAD patterns of the two phases with
(a)—$[111]_W // [011]_{Mg}$; (b)—$[112]_W // [1\bar{2}1]_{Mg}$;
(c)—$[011]_W // [1\bar{2}2]_{Mg}$ and (d)—$[011]_W // [\bar{3}45]_{Mg}$

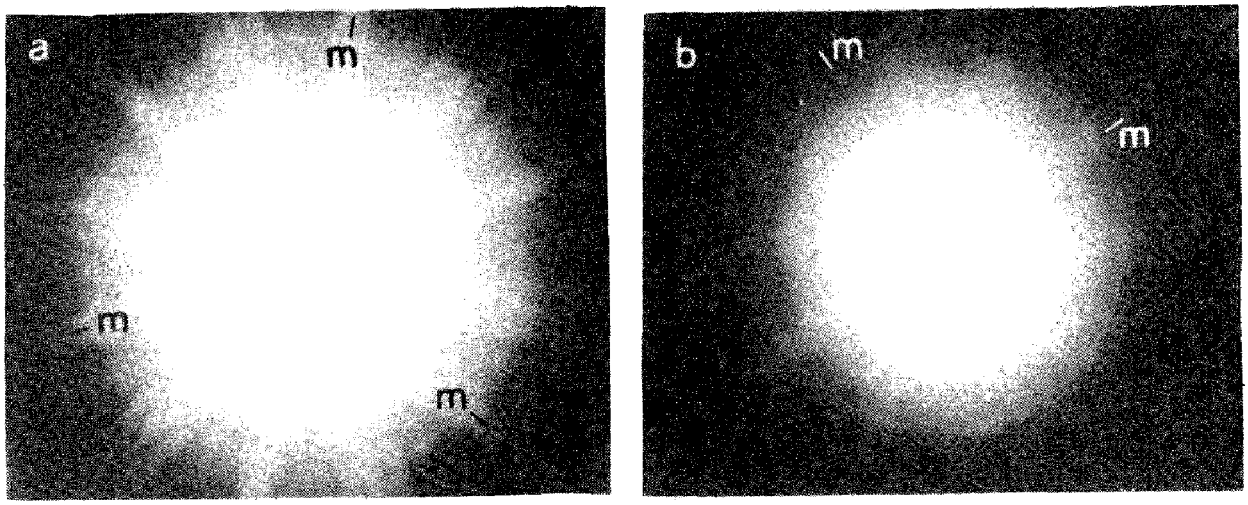

Fig. 7 CBD patterns of W phase at
(a)— $[111]$ zone; (b)— $[011]$ zone

Four space groups correpond to $m3m$ point group. As no evident G-M lines are

present in the diffraction plate of the W pahse at various zones, its space group is $Fm3m$.

The W and W′ phase have the same structure, hence they have the same point and space groups.

4 CONCLUSIONS

(1) The W phase, which distributes along the grain boundaries in the form of a lamellar eutectoid, is of *FCC* structure with $a=0.685$ nm.

(2) The W′ phase with a parameter three times larger than that of the W pahse is found in the alloy containing lower Y content. The W′ and W phase have a simple orientation relationship of $(100)_W // (100)_{W'}$, $(010)_W // (010)_{W'}$, and $(001)_W // (001)_{W'}$.

(3) No orientation relationship was found between the matrix and the W or W′ phases.

(4) The point group of the W and W′ phases is $m3m$ and space group is $Fm3m$.

REFERENCES

1 Raynor, G V. The Physical Metallurgy of Magnesium and Its Alloys. London: Pergamon, 1959.

2 Leontis, T E. In: Spedding. F H and Daane. A H(eds). The Rare Earths. New York: John Wiely sons, Inc. 1961. 455—498.

3 Roberts. C S. Magnesium and Its Alloys. New York: John Wiley Sons Inc. 1960.

4 Emley. E F. Principles of Magnesium Technology. Oxford: Pergamon Press. 1966.

5 Zhang. S Q. Acta metall Sinica. 1990. 3A (2): 110—115.

6 Luo. Z P; Zhang. S Q. In: Kuo. K H; Zhai. Z H(eds). Electron Microscopy 1. Singapore: World Scientific. 1992: 352—353.

7 Drits. M E *et al*. Alloys of Mg with Y. Moscow: Science Press. 1979: 76—93 (in Russian).

8 Padezhnova. E M *et al*. Akademiia Nauk SSSR. Iavestia. Metally. 1979. (1): 217—221 (in Russian).

9 Padezhnova. E M *et al*. Akademiia Nauk SSSR. Izvestiia. Metally. 1982. (4): 201—208 (in Russian).

10 Tao. C H; Zhang. S Q and Lu. L Q. J of the Chinese Rare Earth Society. 1990. 8(2): 150—153.

11 Luo. Z P; Zhang. Z Q; Wei. L G and Lu. L Q. Mat Eng 1992. (7—9): 256—257Q.

12 Wei. Q J. Electron Microstructural Analysis of Materials. Beijing: Metallurgy Industry Press. 1990. 71.